Finite Element Modelling of Electrostatic Fields in Process Tomography Capacitive Electrode Systems for Flow Response Evaluation

S. H. Khan, *Member, IEEE* , and **F. Abdullah**
City University, Department of Electrical, Electronic & Information Engineering
Northampton Square, London EC1V 0HB, UK

Abstract-**This paper describes various aspects and results of 2D finite element (FE) modelling of electrostatic fields in 12-electrode capacitive systems for two-phase flow imaging. The capacitive technique relies on changes in capacitances between electrodes (mounted on the outer surface of the flow pipe) due to the change in permittivities of flow components. The measured capacitances between various electrode pairs and the field computation data are used to reconstruct the cross sectional image of the flow components. FE modelling of the electric field is necessary to optimize design variables and evaluate the system response to various flow regimes, likely to be encountered in practice. Results are presented in terms of normalized capacitances for various flow regimes. The effects of key geometric parameters of the electrode system are also presented and analyzed.**

I. Introduction

In recent years capacitive technique which forms the basis of electrical capacitive tomography (ECT) for imaging and measurement of two-phase flows has gained considerable momentum [1], [2]. The technique involves a number of capacitive electrodes mounted circumferentially around a flow pipe and interrogated in turn by electronic control. Capacitances are measured between various electrode pairs and the data, thus obtained are used to reconstruct the cross sectional image of flow components. Beck et al. [3] first proposed to exploit this technique which has been found to have considerable potential to be used in process industry, especially the oil industry. Hence, the term 'process tomography' has emerged. Recently, sussessful testing of the industrial prototype of a 12-electrode capacitive system [4] has shown the feasibility of this technique for imaging two-phase flows of different permittivities (e. g. oil/gas, oil/water, etc.) in real time. Comparing to other imaging systems capacitive systems are cheap, fast, noninvasive and simple to construct.

The quality of the reconstructed image and the performance of a multielectrode ECT system depend on the uniformity of sensitivity distribution between sensor electrodes which, in turn depends on the inherently nonuniform electric field distribution over the flow pipe cross section. This nonuniformity not only depends upon the geometric and material parameters of the electrode system [5] but also upon the permittivities, distributions and orientations of flow components over the flow pipe cross section. For this reason it is important to be able to investigate the effects of various geometric parameters and flow regimes in order to optimize the electrode system and achieve best system performance in terms of image quality. This is effectively done for a 12-electrode capacitive system by numerical modelling of electric fields by the finite element method (FEM) [6].

II. Constructive Features and the Working Principle of a Multielectrode Capacitive System

Fig. 1 shows the cross section of a 12-electrode capacitive system for ECT flow imaging. It consists of 12 capacitive electrodes mounted symmetrically on the insulating section of a pipeline. The radial screens in between electrodes reduce large capacitances between adjacent electrodes and thereby, increase measurement accuracy. The outer screen with radius R_3 is earthed to shield the electrode system from stray fields. The empty space between this screen and the pipe wall outer surface is filled with dielectric material ($\varepsilon = \varepsilon_{fil}$) which insulates the electrodes from the screen. The inner radius R_1 of the pipe wall ($\varepsilon = \varepsilon_{pw}$) is usually fixed for a given pipeline. The rest of the geometric and material parameters like the electrode angle θ, pipe wall thickness $\delta_1 = R_2 - R_1$, outer screen distance δ_2, radial screen thickness scth, its depth scgp, number of electrodes N, and permittivities ε_{fil} and ε_{pw} can vary.

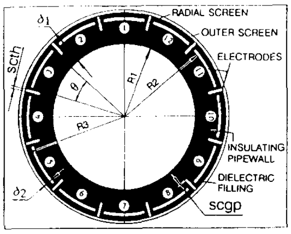

Fig. 1. Cross section of a 12-electrode capacitive system for ECT flow imaging (not in scale).

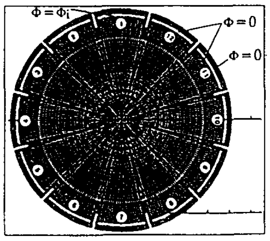

Fig. 2. Finite element model of the 12-electrode capacitive system (full model).

The data acquisition in the above system is carried out by imposing a constant potential to one of the electrodes ('active electrode') and measuring the capacitances between this and rest of the electrodes ('detecting electrodes', kept at zero potential) by discharging the active electrode and measuring the discharging currents (proportional to the unknown capacitances) from the detecting electrodes [1]. For all possible combinations of active and detecting electrodes this process gives a total of $n = N(N-1)/2$ independent capacitance measurements in an N-electrode ECT system. In between a pair of active and detecting electrodes a narrow region of positive sensitivity can be defined within which a unit dielectric increase leads to an increase in their capacitance measurements. The presence of a dielectric material inside this region can thus be detected from measured capacitances. For all different combinations of electrode pairs these narrow regions create the total positive sensing area of the electrode system over the pipeline cross section. A suitable image reconstruction algorithm could be used to exploit the functional relationship between the measured capacitances, dielectric and sensitivity distribution functions and solve the inverse problem of determining the actual flow component distribution [2].

III. Finite Element Modelling of Electric Fields in Multielectrode Capacitive Systems

The electrostatic field in a multielectrode capacitive system shown in Fig. 1 is generated by the active electrode, and the interaction of the field with the dielectric flow components is detected through respective capacitance changes between various electrode pairs. Under corresponding assumptions this field is given by the following Laplace's equation (considering free charge distribution) in terms of electrostatic potential $\Phi = \Phi(x, y)$ in the 2D region Ω of a capacitive electrode system:

$$\nabla.[\varepsilon(x, y) \nabla \Phi(x, y)] = 0 \quad \text{in } \Omega \quad (x, y) \in \Omega \qquad (1)$$

Assumptions: (a) The effects of fringing fields due to the finite length of electrodes are negligible; (b) within the electrode length flow component distribution of a two-phase flow does not change spatially along the axial direction of the pipeline; (c) permittivities of flow components remain constant and do not depend on the field; (d) the dielectric medium in the 2D region Ω is piece-wise homogeneous and isotropic. Under these assumptions and appropriate boundary conditions the 2D FE solution of (1) for given permittivity distributions of flow components $\varepsilon = \varepsilon(x, y)$ gives the electrostatic potential at any point in the region of interest Ω. From this field vectors **E**, **D** and capacitances between the electrodes are calculated. This capacitance C is calculated from the total charge Q distributed on the detecting electrode using $C = Q/V$, where V is the potential difference between the electrodes. The total charge Q is obtained using the Gauss's law [7] given by the following equation:

$$Q = \int_s D_n \, ds = \int_s D\cos\theta \, ds = \int_s \mathbf{D}.\mathbf{n} \, ds = \int_s \mathbf{D}.\mathbf{ds} \qquad (2)$$

From equation (2) it follows that the integral of the normal component of the flux density D_n over any closed surface s enclosing the detecting electrode is equal to the total charge Q distributed on it. If the detecting electrode surface is selected as the surface s then the calculation of Q becomes much easier to perform as there is no need to find D_n since electric field lines are always perpendicular to a conducting surface. In this case $Q = \int_s D \, ds$ which gives $C = (\int_s D \, ds)/V$, where D is the magnitude of vector **D**.

Fig. 2 shows the typical FE model of the electrode system shown in Fig. 1. For this full model, only Dirichlet boundary conditions are used. Specifically, electrode 1 is taken as the active electrode with potential $\Phi = \Phi_i \neq 0$. Rest of the electrodes and the outer screen are kept at zero potential ($\Phi = 0$). Basically, this model is used to simulate electric fields for various two-phase flow regimes shown schematically in Fig. 3. Flow concentrationa β (expressed in %) is given by the ratio of the cross sectional area of the higher permittivity (ε_2) component, S_2 and that of the flow pipe, S_1; namely $\beta = (S_2/S_1)100\%$, where $S_1 = \pi R_1^2$. For the

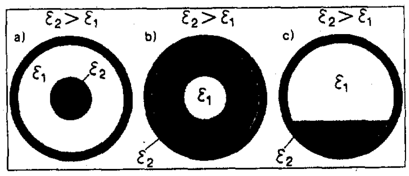

Fig. 3. Various two-phase flow regimes likely to be encountered in practical exploitation of capacitive electrode systems: a) core flow b) annular flow c) stratified flow.

empty pipe and radially symmetrical flow regimes (e.g. core flow, annular flow) electric field distribution inside the flow pipe is symmetrical as shown in Fig. 4. In these cases only a half model of the electrode system with appropriate

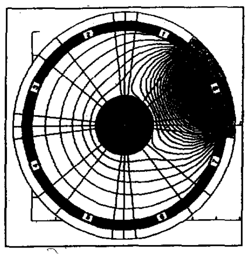

Fig. 4. Equipotential lines in an 8-electrode capacitive system showing symmetry in their distribution (core flow).

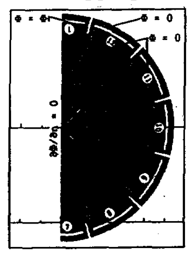

Fig. 5. FE model of the 12-electrode capacitive system considering symmetry in field distributions (half model).

boundary conditions (both Dirichlet and Neumann conditions) needs to be considered (Fig. 5). By adding FE regions with appropriate material properties inside the flow pipe FE models for various flow regimes and concentrations are obtained from the basic models shown in Fig. 2 and 5. Figure 6 shows the FE models for (a) 10%

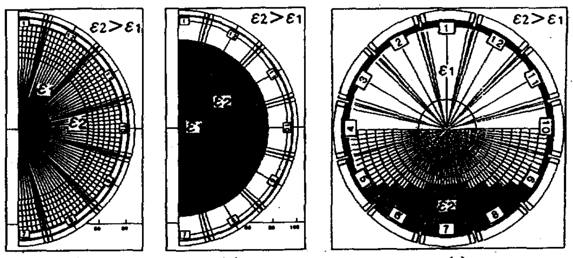

(a) (b) (c)

Fig. 6. FE models for the simulation of various flow regimes: (a) 10% core flow (b) 90% annular flow (c) 21% stratified flow.

core ($\beta = 10\%$), (b) 90% annular and (c) 21% stratified flows. By interchanging the material properties of corresponding FE regions various models for annular flow regimes are obtained from those used for core flows. For stratified flows the orientation of the higer permittivity flow component distribution can be different with respect to a given active electrode.

IV. Results and Discussions

Fig. 7 shows some of the modelling results for various flow regimes discussed above. Results are given in terms of the variation of normalized capacitances with flow concentration β and geometric parameters δ_1 and scgp. Normalized capacitance C^n_{ij} between electrode pair i-j is defined as $C^n_{ij} = (C^p_{ij} - C_{0ij})/(C^f_{ij} - C_{0ij})$ where, C_{0ij}, C^f_{ij} and C^p_{ij} are capacitances between i-j when the flow pipe is empty ($\beta = 0$, $\varepsilon = \varepsilon_1 = 1$), full of material of $\varepsilon = \varepsilon_2$ ($\beta = 100\%$)

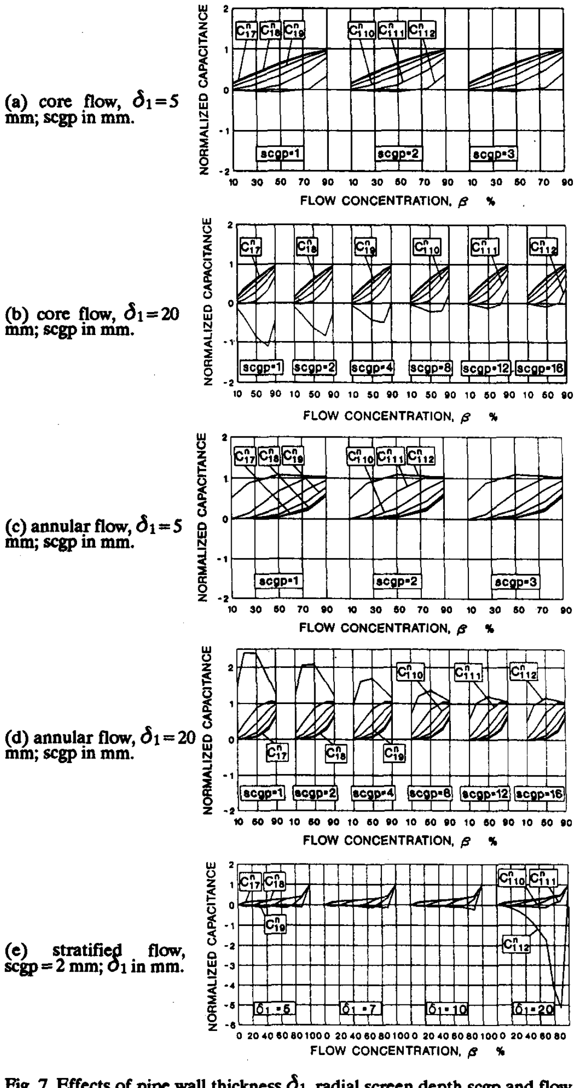

Fig. 7. Effects of pipe wall thickness δ_1, radial screen depth scgp and flow concentration β on normalized capacitances.

and has a two-phase flow of given concentration $\beta \neq 0$ ($\varepsilon_1 = 1$, $\varepsilon_2 > 1$) respectively. Normalized capacitance is one of the main performance parameters of capacitive electrode systems. To avoid saturation of sensor electronics due to large capacitance changes and ensure good quality image reconstruction it is desirable to limit the values of these capacitances so that $0 \leq C^n_{ij} \leq 1$ [2]. Fig. 7 clearly reflects the effects of flow regimes and concentrations (β) and the geometric parameters of the electrode system (δ_1, scgp) on normalized capacitances which, eventually determine the image quality. For thin pipe wall electrode systems (Fig. 7a, c and e) these capacitances mostly remain between 0 and 1 (especially for core and annular flows) and do not depend on β and scgp. However, for thick pipe wall electrode systems with small scgp (Fig. 7b, d and e) large capacitances are observed between adjacent electrodes C^n_{112} (electrode 1 is the active electrode). This is especially evident in the case of stratified flows (Fig. 7e) for which even larger C^n_{112} have been obtained for some orientations of the higher permittivity flow component [8]. As can be seen from Fig. 7b and d, for a given δ_1, high normalized capacitances between adjacent electrodes can be reduced by appropriately choosing the radial screen depth scgp.

V. Conclusions

One of the vital performance parameters of a 12-electrode capacitive system for ECT flow imaging has been investigated by FE modelling of electric fields. Various results have shown the effectiveness of the adopted modelling approach (validated by experiments [9]) for the CAD and performance evaluation of these systems.

Acknowledgment

The authors would like to thank SERC, UK for financing this work under an SERC grant, Professor M. S. Beck and Dr. C. G. Xie from UMIST and Dr. S. M. Huang from the Schlumberger Cambridge Research Limited, UK for their long standing collaboration.

References

[1] S. M. Huang, C. G. Xie, R. Thorn, D. Snowden, and M. S. Beck, "Design of sensor electronics for electrical capacitance tomography," **IEE Proceedings-G**, vol. 139, no. 1, pp. 83-88, 1992.

[2] C. G. Xie, S. M. Huang, B. S. Hoyle, R. Thorn, C. Lenn, D. Snowden, and M. S. Beck, "Electrical capacitance tomography for flow imaging: system model for development of image reconstruction and design of primary sensors," **IEE Proceedings-G**, vol. 139, no. 1, pp. 89-98, 1992.

[3] M. S. Beck, A. Plaskowski, and R. G. Green, "Imaging for measurement of two-phase flows," in VERET, C. (Ed.): Flow Visualization IV, **Proc. 4th Int. Symposium on Flow Visualization**, pp. 585-588, 1986.

[4] M. S. Beck, B. S. Hoyle, and C. P. Lenn, "Process tomography in pipelines," **SERC Bulletin**, vol. 4, no. 10, pp. 24-25, 1992.

[5] S. H. Khan and F. Abdullah, "Computer aided design of process tomography capacitance electrode systems for flow imaging," in **Sensors: Technology, Systems and Applications**, Ed. K. T. V. Grattan, Bristol: Adam Hilger, 1991, pp. 209-214.

[6] P. P. Silvester and R. L. Ferrari, **Finite Elements for Electrical Engineers**, 2nd ed., Cambridge: Cambridge University Press, 1990.

[7] S. Ramo, J. R. Whinnery, and T. V. Duzer, **Fields and Waves in Communication Electronics**, New York: John Wiley & Sons, Inc., 1965, p. 754.

[8] S. Umashangar, "A study of the system response to stratified flow for a 12-electrode flow imaging system using finite element method," B.Eng Project Report, City University, London, 1992.

[9] S. H. Khan and F. Abdullah, "Validation of finite element modelling of multielectrode capacitive system for process tomography flow imaging," in **Proc. Europ. Concerted Action on Process Tomography**, Manchester, March 1992, pp. 29-39.